Environmental Science & Technology

Article

Cite This: Environ. Sci. Technol. XXXX, XXX, XXX−XXX

pubs.acs.org/est

Rate-Limiting Mass Transfer in Micropollutant Degradation Revealed by Isotope Fractionation in Chemostat

Benno N. Ehrl,[†] Kankana Kundu,*[,†] Mehdi Gharasoo,[†] Sviatlana Marozava,[†] and Martin Elsner*[,†,‡]

[†]Institute of Groundwater Ecology, Helmholtz Zentrum München, Ingolstädter Landstrasse 1, 85764 Neuherberg, Germany

[‡]Chair of Analytical Chemistry and Water Chemistry, Technical University of Munich, Marchioninistrasse 17, 81377 Munich, Germany

Supporting Information

ABSTRACT: Biodegradation of persistent micropollutants like pesticides often slows down at low concentrations (μg/L) in the environment. Mass transfer limitations or physiological adaptation are debated to be responsible. Although promising, evidence from compound-specific isotope fractionation analysis (CSIA) remains unexplored for bacteria adapted to this low concentration regime. We accomplished CSIA for degradation of a persistent pesticide, atrazine, during cultivation of *Arthrobacter aurescens* TC1 in chemostat under four different dilution rates leading to 82, 62, 45, and 32 μg/L residual atrazine concentrations. Isotope analysis of atrazine in chemostat experiments with whole cells revealed a drastic decrease in isotope fractionation with declining residual substrate concentration from $\varepsilon(C) = -5.36 \pm 0.20‰$ at 82 μg/L to $\varepsilon(C) = -2.32 \pm 0.28‰$ at 32 μg/L. At 82 μg/L $\varepsilon(C)$ represented the full isotope effect of the enzyme reaction. At lower residual concentrations smaller $\varepsilon(C)$ indicated that this isotope effect was masked indicating that mass transfer across the cell membrane became rate-limiting. This onset of mass transfer limitation appeared in a narrow concentration range corresponding to about 0.7 μM assimilable carbon. Concomitant changes in cell morphology highlight the opportunity to study the role of this onset of mass transfer limitation on the physiological level in cells adapted to low concentrations.

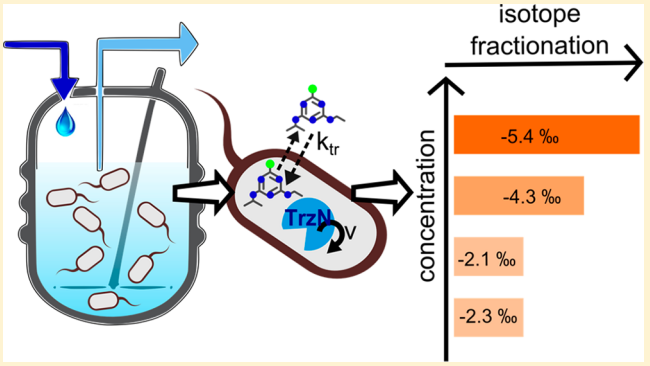

INTRODUCTION

Assessing the biodegradation of anthropogenic micropollutants is a prominent challenge of our time. Industrial chemicals,[1] disinfectant byproducts,[2] pharmaceuticals,[3] personal care products,[4] and pesticides[5,6] are released ubiquitously from nonpoint sources. They are detected with increasing frequency at trace concentrations (ng/L to μg/L) in the environment with the potential to impact ecosystems and human health.[7,8] Assessing and understanding their degradation raises two aspects of fundamental importance: first, the identification of the limits of biodegradation and second, an in situ assessment of biodegradation.

First, micropollutants are often quite persistent,[9] not only because nonpolar micropollutants can initially sorb to soil and sediment,[10] but also because their biodegradation is observed to slow and ultimately stall below concentrations of 1−100 μg/L.[11] How exactly bacteria adapt to low concentrations, however, is an open question. Do they maintain high degradation rates so that, at one point, mass transfer becomes slow relative to enzymatic turnover? Then organisms would inevitably run into bioavailability limitations at low concentrations.[12−14] Or does enzymatic breakdown slow down so that biotransformation is never truly mass-transfer limited?[15] Then an opportunity may arise to intervene, delay this adaptation and, hence, push degradation toward lower levels. A current obstacle for management and natural attenuation strategies is therefore a knowledge gap of the true limitations in pollutant degradation at very low concentrations. Second, it is a challenge to confidently detect biodegradation in complex natural systems. Environmental micropollutant concentrations decrease not only due to degradation, but also by physical processes (diffusion, sorption, transport). Concentration analysis alone is, therefore, often not sufficient to quantify biodegradation in situ and alternative approaches are warranted

To address the second aspect − quantifying micropollutant biodegradation in situ − compound-specific isotope analysis offers such an alternative approach, because information on degradation is not derived from concentrations, but instead from stable isotope ratios of a pollutant. Due to the isotope effect of enzymatic reactions, biodegradation leads to changes in isotope ratios (usually an enrichment of heavy isotopes) at their natural abundance in the remaining pollutant mole-

Received: September 13, 2018
Revised: December 3, 2018
Accepted: December 5, 2018
Published: December 5, 2018

DOI: 10.1021/acs.est.8b05175
Environ. Sci. Technol. XXXX, XXX, XXX−XXX

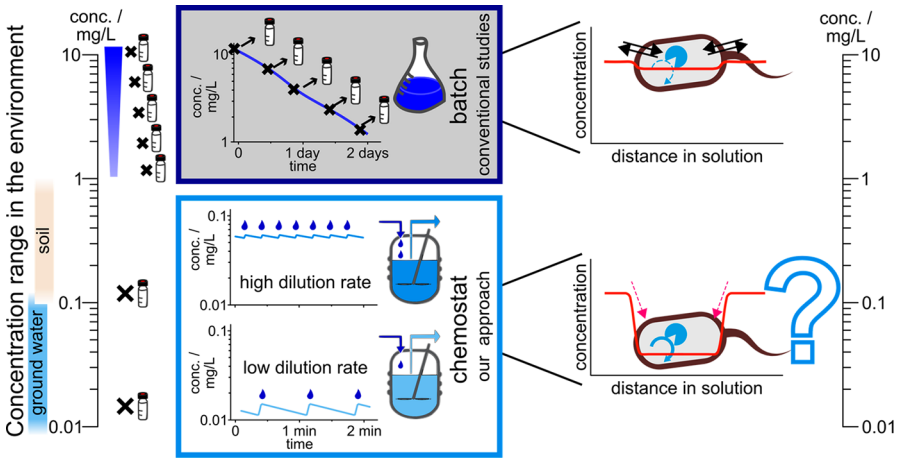

Figure 1. Conventional isotope fractionation studies have been conducted at high concentrations, whereas the chemostat approach allows measuring isotope fractionation at low, environmentally relevant concentrations (left) which allows to detect mass transfer limitations (right). Typical pesticide and pharmaceutical concentrations in the environment are in the μg/L to subμg/L regime, whereas laboratory-based batch studies have consistently investigated degradation-associated isotope fractionation at much higher (mg/L) concentrations (upper panel). Chemostat experiments (lower panel) close the gap by achieving distinct, small steady-state concentrations through varying the dilution rate. Our numerical modeling (modeled residual atrazine concentrations in the lower panel concentration graphs) validates the approach by demonstrating that the oscillation of the residual substrate concentration—resulting from dropwise addition of the media—is negligible. While at high concentrations, mass transfer is not rate limiting for atrazine biodegradation, a different situation could arise at low concentrations, when the enzymatic turnover is faster than the cellular atrazine is replenished by passive permeation of the cell envelope.

cules.[16] Changes in isotope ratios of the original contaminant can, therefore, provide evidence as "isotopic footprints" of ongoing biodegradation (or chemical transformation) at contaminated sites, whereas diffusion in water causes much smaller isotope effects.[17−19]

However, isotope fractionation is also informative to study the first aspect−whether biodegradation is limited by mass transfer. As known from photosynthesis,[21−24] sulfate reduction,[25,26] or nitrate reduction[27] the masking of enzyme-associated isotope fractionation can be a unique indicator of diffusion/mass transfer limitation in natural transformations. When mass transfer across a cell membrane becomes increasingly rate-limiting, molecules experiencing the isotopic discrimination in the cytosol are immediately consumed and do not get out of the cell any longer to make the enzyme's isotope effect visible in the bulk solution where samples are taken for isotope analysis. As diffusion in the aqueous phase exhibits a very small isotope effect, the degradation-associated isotope fractionation is masked and decreases.[20,21] This phenomenon has primarily been investigated for substrates that were *not* limiting for growth such as $^{13}C/^{12}C$ in CO_2,[21,23,24] $^{15}N/^{14}N$ in nitrate[27,28] or $^{34}S/^{32}S$ in sulfate[25,26] at elevated concentrations. In contrast, no study so far has been conducted for organic compounds as only growth/energy substrate at low concentrations ("micropollutants"). As recently demonstrated, some small organic compounds (e.g., pesticides) can permeate bacterial cell membranes just by passive diffusion, even without active transport[29,30] in a similar way as CO_2 during photosynthesis.[21,23,24,31] Recent studies highlight the importance of microbial cell envelope on observable isotope fractionation[36] in particular on passive permeation rates of atrazine uptake during biodegradation.[30]

An entirely different twist to the story—which highlights the need to explore degradation specifically at low concentrations—has been brought forward by a conceptual model by Thullner et al.[37,38] The authors demonstrated that the same process—biodegradation of a given compound by a given bacterium—may show large isotope fractionation at high concentrations, however small isotope fractionation at low concentrations. Maybe surprisingly, the large number of studies that have reported pronounced observable isotope fractionation in organic contaminant degradation[32−34] imply that[35] such diffusive mass transfer is frequently *not* rate-limiting at high concentrations.[29] A turning point in isotope fractionation may be expected, however, when substrate availability becomes so low that enzyme binding sites are no longer fully saturated. Whereas enzyme saturation at high substrate concentrations ($c \gg K_M$) implies that enzyme kinetics follows pseudo zero-order and is, therefore, rate-determining, at low concentrations ($c < K_M$) enzyme kinetics essentially becomes a pseudo first-order kinetics process (where K_M is the Michaelis−Menten constant of the enzyme/the Monod-constant of associated microbial growth).[45] Hence, mass transfer can become rate-limiting at low concentrations if (first-order) diffusive exchange is slower than (pseudo-first order) enzymatic turnover. This, in turn, means that the isotope effect of the enzyme reaction will cease to be observable, in exactly the same manner as hypothesized for an onset of bioavailability limitations (see above). This has two consequences. First, if mass transfer limitations prevail at low concentrations, a decrease in isotope fractionation is expected to give direct evidence of this "turning point" so that isotope fractionation bears unique promise as a diagnostic tool to detect the onset of mass transfer limitations at low concentrations.[37,38] Second, however, it means that such low masked isotope fractionation cannot be used to accurately assess the true turnover of trace concentrations in natural systems!

Whether or not such a turning point in isotope fractionation is really observable does not only depend on K_M, but also on microbial adaptation: do bacteria run into mass transfer limitations, or do they adapt their physiology early on (for example by changing cell-wall properties or regulating enzyme expression and activity)? As shown in Figure 1, practically all

DOI: 10.1021/acs.est.8b05175
Environ. Sci. Technol. XXXX, XXX, XXX−XXX

available experimental studies on organic compound transformation have been conducted in batch where concentrations changed over time so that bacteria could never truly adapt to a constant surrounding concentration. In addition, experiments were conducted at high (>1 mg/L) pollutant concentrations because of the substantial substance amount required when multiple samples need to be withdrawn for isotope analysis. The low concentration range in the environment (μg/L; where possible mass transfer limitations are expected to become more severe[38]), in contrast, is practically unexplored territory when it comes to isotope fractionation.[39]

This study, therefore, sets out with a new approach and aims to measure isotope fractionation of micropollutants through cultivating atrazine-degrading bacteria in chemostats (Figure 1). By lowering the dilution rate, environmentally relevant steady-state atrazine concentrations and growth rates can be established and varied to pinpoint the onset of mass transfer limitations. Further, sufficient amounts of sample may be withdrawn at steady-state to facilitate isotope analysis. Finally, bacteria can adapt to low concentrations mimicking carbon- and nitrogen-limiting conditions in the environment. Our model microorganism is the pesticide-degrading bacterium *Arthrobacter aurescens* TC1, which grows on atrazine as sole carbon and nitrogen source.[40] Hydrolysis by the cytoplasmic enzymes (TrzN, AtzB, and AtzC) first leads to 2-hydroxyatrazine and subsequently produces cyanuric acid, while the alkylamine side chains are further mineralized or used to build up biomass as shown in the Supporting Information (SI) Figure S1.[41] Strong isotope fractionation during the degradation of atrazine with whole cells[32] and the purified recombinant enzyme[35] indicate that mass transfer is not rate-limiting at high concentrations. Also, an analogue of TrzN (AtzA) has been reported to be constitutively expressed in batch experiments at high initial concentrations of atrazine at early and later exponential phase.[42,43] Absence of down-regulation of s-triazine hydrolases at low atrazine concentrations would mean that enzyme activity stays high, making *A. aurescens* TC1 a suitable organism to explore an onset of mass transfer limitations. Conversely, if expression of TrzN were to be regulated at low concentrations, *A. aurescens* TC1 would again be well suited to explore this effect. Together, this makes *A. aurescens* TC1 an ideal model organism to pioneer the study of its isotope fractionation in chemostat cultivation and to explore limitations of micropollutant biodegradation at trace concentrations. This novel strategy was accompanied by numerical modeling of the chemostat cultivation to validate the experimental approach. A more detailed description of the model can be found in Gharasoo et al.[44]

EXPERIMENTAL SECTION

Continuous Cultivation. The atrazine degrading bacterium *A. aurescens* TC1 was cultivated in a glass bioreactor (diameter 130 mm, height 250 mm, and working volume 2000 mL; Applikon Biotechnologie B.V., Netherlands). The cultivation was controlled by myControl (Applikon Biotechnologie B.V., Netherlands) and samples for flow cytometry, concentration analysis by HPLC-UV-DAD, and isotope analysis were taken through the reactor's sampling tube. The cultivation media was a mineral salt medium with 30 mg/L atrazine (97%, Cfm Oskar Tropitzsch, Germany) as sole carbon and nitrogen source. When the bioreactor was initially started in batch mode, also the inoculum (10%) was prepared with mineral salt medium (with total organic carbon content <10 μg/L to prevent carry-over of carbon) supplemented with solid atrazine in excess. The media preparation and the culture conditions are described in the SI. Because atrazine was in large excess of any other organic carbon content present in the feed (<10 μg/L), and because impurities from the walls of the chemostat vessel would be quickly washed out in continuous-flow mode, significant alternative carbon sources are not expected. The bacteria were cultivated over a total cultivation time of 140 days at different dilution rates of μ = 0.023 h^{-1}, 0.018 h^{-1}, 0.009 h^{-1}, and 0.006 h^{-1} to adjust different growth rates and different concentrations of residual atrazine in the bioreactor.

Calculations to Describe Mass Transport Across the Cell Envelope during Chemostat Cultivation. A numerical model was developed to assess the influence that mass transfer limitations exert on the observed isotopic signature at low steady state concentrations in the chemostat. This model simulates the atrazine degradation, growth, and isotope fractionation in the presence of rate-limiting mass transfer with a mass transfer coefficient k_{tr}[45] and can be extended to include maintenance energy (see SI). The kinetic growth parameters for the model were derived from the different dilution rates of the chemostat run (Kundu et al., in communication) and a fed batch growth experiment (SI Figure S4). With a high time resolution of the model, the influence of subsequent droplet addition with the media feed can be analyzed, was found to be negligible under our operating conditions and may only become of relevance at a dilution rate lower than μ = 0.004 h^{-1} (Figure 1, Figure 3A). The model itself has a broader application range which goes beyond the scope of this study. A detailed description of the model and the code can be found in Gharasoo et al.[44]

The diffusion coefficient through the membrane D_{mem} and the apparent permeability of the cell wall P_{app} can be calculated according to eq 1 where V_{out} is the bioreactor volume (2000 mL)

$$D_{mem} = P_{app}\frac{w}{K_{lipw}} = \frac{k_{tr} \times V_{out} \times w}{A_{cells} \times K_{lipw}} \quad (1)$$

minus the total cell volume (V_{cells}). V_{cells} and A_{cells}—total volume and surface area of all cells—are calculated by the product of the total number of living cells in the bioreactor (4×10^{10}) (Figure 2C) and the volume, or surface area of a single cell (1.9×10^{-16} m^3, or 3.6×10^{-12} m^2), respectively. The area and the volume of a single cell are calculated assuming a cylindrical shape (Figure 2D). K_{lipw} = 741 is the lipid–water distribution coefficient of atrazine[46] and $w = 4 \times 10^{-9}$ m is a typical value for the membrane thickness.[47]

Calculation of Enrichment Factors in Chemostat. The classical way to determine the enrichment factor of a contaminant degradation reaction relies on the Rayleigh equation where changes in isotope ratios are monitored with decreasing substrate concentration.[48] Alternatively, studies may assess the difference in isotope values of substrate and product when out of large pool of substrate only a small fraction is transformed to one specific product (e.g., biomass out of CO_2 or sulfide out of SO_4^{2-}). Both approaches are not possible in micropollutant degradation when >99% of the substrate is transformed, metabolites may be further degraded, may not be accessible to compound specific isotope analysis, or may not even be detectable at all. When studying micropollutant degradation in bioreactors at constant, steady state

DOI: 10.1021/acs.est.8b05175
Environ. Sci. Technol. XXXX, XXX, XXX−XXX

concentrations the enrichment factor of the degradation of atrazine must therefore be determined in a different way. The substrate inflow per time $(F)_{in} = c_{in} \times \mu$ is equal to the outflow per time $(F)_{out} = c_{SS} \times \mu$ plus the substrate degraded per reactor volume V per time $-r = ({}^{dn}/_{dt}/V)$ (eq 2)

$$(F)_{in} = (F)_{out} - r \tag{2}$$

$$c_{in} \cdot \mu = c_{SS} \cdot \left(\mu - \frac{r}{c_{SS}}\right) \tag{3}$$

where c_{in} is the atrazine concentration in the inflow, c_{SS} is the steady-state atrazine concentration in the bioreactor and μ is the dilution rate. In chemostat at low growth rates c_{SS} is typically by a factor of 100−1000 smaller compared to c_{in}.[49,50] Hence, $-r/c_{SS}$ must be much greater than μ meaning that

$$c_{in} \cdot \mu \approx c_{SS} \cdot \left(-\frac{r}{c_{SS}}\right) \tag{4}$$

Stating eq 4 for heavy and light isotopes respectively, and dividing the equations by each other gives an expression for the isotope ratio ${}^{h}c/{}^{l}c$

$$\left(\frac{c^h}{c^l}\right)_{in} \approx \left(\frac{c^h}{c^l}\right)_{SS} \cdot \frac{{}^{h}\left({}^{-r}/_{c_{SS}}\right)}{{}^{l}\left({}^{-r}/_{c_{SS}}\right)} \tag{5}$$

In a first-order process $(-r) = k \cdot c_{SS}$ so that ${}^{h}\left({}^{-r}/_{c_{SS}}\right) = {}^{h}k$ and ${}^{l}\left({}^{-r}/_{c_{SS}}\right) = {}^{l}k$ giving

$$\left(\frac{{}^{h}c}{{}^{l}c}\right)_{in} \approx \left(\frac{c^h}{c^l}\right)_{SS} \cdot \alpha \tag{6}$$

with $\alpha = {}^{h}k/{}^{l}k$.

For a Monod-type growth the expressions ${}^{h}\left({}^{-r}/_{c_{SS}}\right) = \frac{{}^{h}\left({}^{q_{max}}/_{K_M}\right)}{1 + {}^{l}c_{SS} / {}^{l}(K_M) + {}^{h}c_{SS} / {}^{h}(K_M)}$ and ${}^{l}\left({}^{-r}/_{c_{SS}}\right) = \frac{{}^{l}\left({}^{q_{max}}/_{K_M}\right)}{1 + {}^{l}c_{SS} / {}^{l}(K_M) + {}^{h}c_{SS} / {}^{h}(K_M)}$ apply with q_{max} as maximum substrate turnover and K_M as Monod constant. Hence, also here eq 6 is obtained with the only difference that the fractionation factor does not reflect the isotope effect on first order kinetics, but on Monod kinetics, $\alpha = \frac{{}^{h}\left({}^{q_{max}}/_{K_M}\right)}{{}^{l}\left({}^{q_{max}}/_{K_M}\right)}$.

Introducing the more common δ notation

$$\frac{\left(\frac{c^h}{c^l}\right)_x}{\left(\frac{c^h}{c^l}\right)_{ref}} = \delta_x + 1 \tag{7}$$

where $\left(\frac{c^l}{c^h}\right)_x$ and $\left(\frac{c^h}{c^l}\right)_{ref}$ are isotope ratios of the sample and an international standard material gives

$$\delta_{in} + 1 \approx (\delta_{SS} + 1) \cdot \alpha = (\delta_{SS} + 1) \cdot (\varepsilon + 1) \tag{8}$$

where $\varepsilon = \alpha$-1 is the enrichment factor, or isotope fractionation.[51] Finally, ε can be calculated by the difference of the isotope values of inflow and bioreactor because $\delta_{SS} \ll 1$:

$$\varepsilon = \frac{\delta_{in} + 1 - (\delta_{SS} + 1)}{\delta_{SS} + 1} \approx \delta_{in} - \delta_{SS} \tag{9}$$

Hence, irrespective of the kinetics assumed, isotope values of atrazine in the outflow of chemostats are expected to differ from those of the inflow in good approximation by the enrichment factor ε provided that most of the contaminant is degraded and provided that this enrichment factor of the enzyme reaction is not masked by mass-transfer limitations.

Compound Specific Isotope Analysis of Atrazine in the Bioreactor. For each dilution rate (0.023 h^{-1}, 0.018 h^{-1}, 0.009 h^{-1}, and 0.006 h^{-1}) samples for isotope analysis (100 mL, 200 mL, 300 mL, and 500 mL respectively) were withdrawn from the bioreactor (1 sample per bioreactor and dilution rate) after three hydraulic retention times at steady-state had passed. After sampling the bioreactor cultivation continued in fed-batch mode until the initial chemostat volume was reached again. Degradation of the sample was stopped immediately by sterile filtration with a regenerated cellulose membrane filter (pore size 0.2 μm, diameter 47 mm; GE Healthcare ltd., UK). Immediate removal of the degrading cells is necessary, since the atrazine would otherwise be degraded within minutes. Degradation time courses with fresh sample demonstrated that during our sampling time of 1 min, only 10% at most of the remaining atrazine was degraded (SI Figure S5). After filtration, the atrazine was extracted with dichloromethane (10% of the sample volume, three times).[32] The dichloromethane was evaporated under a nitrogen stream and the atrazine was reconstituted in 100 μL ethyl acetate. Simultaneously, 1 mL of the inflow to the chemostat was collected (which was sufficient because of the high feed concentration) frozen at −80 °C, dried by lyophilization, and the atrazine was reconstituted in 100 μL ethyl acetate, as well. Carbon and nitrogen isotope analyses of atrazine were performed on a GC-IRMS system consisting of a TRACE GC Ultra gas chromatograph (Thermo Fisher Scientific, Italy) equipped with a DB-5 analytical column (60 m, 0.25 mm i.d., 1.0 μm film, Agilent Technologies, Germany) coupled to a Finnigan MAT 253 isotope ratio mass spectrometer via a Finnigan GC Combustion III interface (both Thermo Fisher Scientific, Germany). Detailed information about the method adapted from Schreglmann et al.[52] is provided in the SI.

Concentration Measurements, Cell Counting, and Microscopy. Atrazine and 2-hydroxyatrazine concentrations were measured using a Prominence HPLC system (Shimadzu Corp., Japan) together with a 100 × 4.6 mm Kinetex 5 μ Biphenyl 100 Å column (Phenomenex Inc., Golden, CO). For cell counts, cells were first fixed with 2.5% glutaraldehyde, then stained with SYBR Green I (total cells) and propidium iodide (dead cells) and analyzed on a Cytomics FC 500 flow cytometer (Beckmann Coulter, Hebron, KY). The shape of fixed cells was analyzed on agar glass slides by light microscopy with an Axioscope 2 Plus microscope (Carl Zeiss AG, Germany). For a detailed description of these methods see the SI.

Statistical Treatment of Concentration and Isotope Data. The chemostat culture was performed in two biological replicates. The steady state concentrations of the individual biological replicates measured during the last 4 days of each dilution rate were compared with a two sample t test ($N = 4$). As they were not statistically different from one another at the 0.05 level for each dilution rate, the concentration values were combined and the average substrate concentration and the standard error for each dilution rate were calculated ($N = 8$). A similar approach was chosen for the determination of the enrichment factors. The enrichment factor for each biological

DOI: 10.1021/acs.est.8b05175
Environ. Sci. Technol. XXXX, XXX, XXX−XXX

replicate at each dilution rate was determined as described above in five technical replicates per bioreactor sample which were compared with a two sample *t* test ($N = 5$). As they were not statistically different from one another at the 0.05 level for each dilution rate, the enrichment factors of the two biological replicates were combined and the average and the 95% confidence intervals were calculated for each dilution rate ($N = 10$).

RESULTS AND DISCUSSION

Studying Isotope Fractionation of Atrazine Degradation at Low Substrate Concentrations in Chemostats. We established a new approach to explore isotope fractionation during micropollutant degradation by microorganisms adapted to trace contaminant concentrations by cultivating the atrazine degrader *A. aurescens* TC1 in chemostats (Figure 1). By lowering the dilution rates in the chemostats stepwise (from 0.023 h^{-1} to 0.006 h^{-1}), environmentally relevant steady-state concentrations of pollutants were established (32 μg/L at the lowest dilution rate) and these concentrations were varied to probe for the concentration where the mass transfer across the cell envelope becomes rate limiting for the biodegradation of atrazine. The chemostat approach allowed withdrawing sufficient amounts of sample at steady-state to facilitate isotope analysis. Simultaneously, bacteria could adapt to low substrate concentrations.[11]

Aerobic cultivation of *A. aurescens* TC1 in chemostat at a high dilution rate (0.023 h^{-1}; t = 19 days; SI Figure S2) resulted in a steady state residual atrazine concentration of 82.6 ± 2.0 μg/L meaning that more than 99.8% of the atrazine of the inflow (30 mg/L) was transformed into the final product cyanuric acid. Also hydroxyatrazine concentrations (between 67 and 256 μg/L in all experiments) made up only between 0.1% and 0.6% of the mass balance and the subsequent metabolite *N*-isopropylammelide was not detected. The predominant downstream product was cyanuric acid confirming that, as expected, degradation of atrazine involved mineralization of the side chains to over 99%, whereas the aromatic ring was left untouched. These residual concentrations of atrazine (82 μg/L equals 0.4 μM) and hydroxyatrazine (between 67 and 256 μg/L, respectively 0.3 and 1.3 μM) are already considered as substrate limitation[11,53] and are also found in U.S. groundwater close to atrazine treated maize plots.[54] The isotopic signature of atrazine in the bioreactor showed a difference of $\delta^{13}C_{in} - \delta^{13}C_{SS} \approx \varepsilon(C) = -5.36 \pm 0.20‰$ compared to the inflow, which—as we predict (see theoretical treatment in the Experimental Section)—is identical to the enrichment factors determined in high concentration batch degradation with resting cells[32] and pure enzyme.[35] This strong isotope fractionation demonstrates that the degradation is not (yet) mass transfer limited at 82 μg/L (0.38 μM) residual atrazine concentration. Our determination of isotope fractionation in chemostats bears considerable novelty. A limited number of previous chemostat studies evaluated isotopic differences between substrate and product.[21,23,24,55,56] This approach, however, is restricted to exceptional cases, since it requires that most of the substrate remains unreacted and only a small fraction is turned over (such as in photosynthesis[21,23,24] or methanogenesis from a large pool of CO_2/bicarbonate[57] or in sulfide production from a large pool of sulfate[55]). These reactant-product comparisons do not work for growth-limiting substrate, since at steady-state these substrates (atrazine in our case) are turned over to more than 99%. For reasons of mass balance, the isotope ratio of the biomass or CO_2—as predominant anabolic and catabolic products of atrazine—would show the initial isotope ratio of the atrazine feed. Hence, it is necessary to measure the isotope ratio of the standing stock of residual atrazine to determine the degradation-associated isotope fractionation as derived in eqs 2−9. For a more detailed consideration of isotope fractionation in steady-state turnover see also the seminal treatment by Hayes.[58] To our knowledge this is the first chemostat experiment which determines isotope enrichment factors with high precision by measurements of the same limiting substrate in inflow and outflow of a bioreactor. This expands chemostat-based isotope fractionation studies to a large number of target compounds including all cases where a substrate is truly limiting for growth and where the isotope ratio of immediate products cannot be determined (because ε−values are derived from isotope analysis of the substrate only). This chemostat approach has two advantages over batch reactions. First, the result does not depend on concentration measurements, which makes it more precise as no error is introduced by the concentration measurements. Second a one-time sampling at steady state makes studies at low concentration accessible, where fast degradation or low solubility would not allow withdrawing multiple large-volume samples over time in batch experiments, as needed for typical evaluations of ε(C) by the Rayleigh equation.[48,59]

Mass Transfer Limitations Revealed by Isotope Fractionation. We exploited this new opportunity to investigate if, and at what point, mass transfer became limiting when atrazine concentrations were systematically lowered by decreasing dilution rates (μ_{med} = 0.018 h^{-1}, μ_{low} = 0.009 h^{-1}, and μ_{min} = 0.006 h^{-1}) over a total cultivation time of 120 days (Figure 2). As expected, these lower dilution rates resulted in lower respective residual atrazine concentrations of 61.5 ± 1.3 μg/L (0.29 μM) at μ_{med}, 44.5 ±1.0 (0.20 μM) at μ_{low}, and 31.9 ± 1.0 μg/L (0.15 μM) at μ_{min}; Figure 2B). Remarkably, these low-concentration experiments also resulted in a dramatic decrease in isotope fractionation compared to batch studies with resting cells,[32] pure enzyme[35] or to chemostat at 83 μg/L (Figure 2A). The concentration-dependent decrease in isotope fractionation is fully consistent with the working hypothesis of mass-transfer limitations at low concentrations, and with predictions by Thullner et al.[37,38] Specifically, the degradation-induced normal carbon isotope effect $((d^{13}C/dt)/(d^{12}C/dt) < 1)$ decreased with lower concentrations to a similar extent (from $\varepsilon(C) = -4.34 \pm 0.13‰$ at μ_{med} to $-2.12 \pm 0.08‰$ at μ_{low} and $-2.32 \pm 0.28‰$ at μ_{min}) as the simultaneously occurring inverse nitrogen isotope effect $((d^{15}N/dt)/(d^{14}N/dt) > 1)$, which decreased from $\varepsilon(N) = 1.94 \pm 0.06‰$ to $1.04 \pm 0.09‰$ and $1.27 \pm 0.08‰$ at corresponding dilution rates. This identical masking despite an opposing nature of the isotope effects was also represented in the dual element isotope trend λ defined by the ratio $\varepsilon(N)/\varepsilon(C)$. Lambda remained constant with decreasing concentration and dilution rate (-0.45 ± 0.13 at μ_{med}, -0.49 ± 0.15 at μ_{low}, and -0.55 ± 0.15 at μ_{min}) and was similar to previous resting cell and pure enzyme degradation experiments (-0.61 ± 0.06 and -0.54 ± 0.02).[35] Taken together, this provides compelling evidence that the underlying enzymatic degradation mechanism (including all steps until irreversible C−Cl bond cleavage) remained the same so that changes in enrichment factors must result from another preceding rate-limiting step masking the isotope fractionation of the

DOI: 10.1021/acs.est.8b05175
Environ. Sci. Technol. XXXX, XXX, XXX−XXX

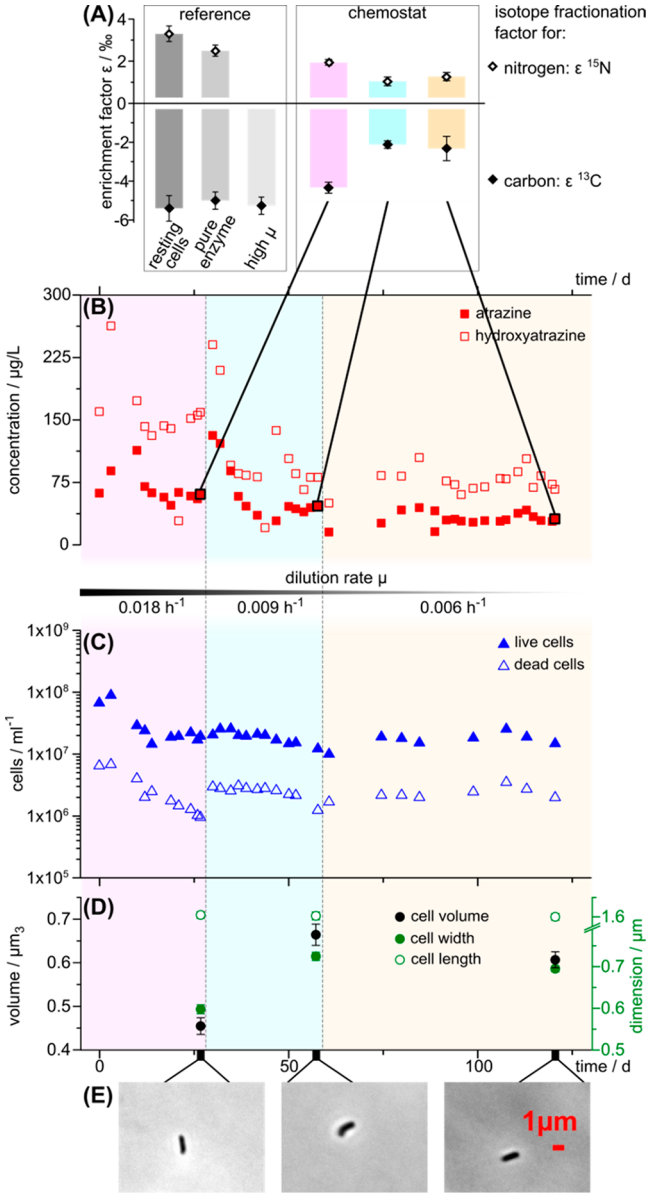

Figure 2. Isotope fractionation of atrazine and associated cell parameters of *A. aurescens* TC1 when cultivated in aerobic, atrazine limited chemostat with stepwise decreased dilution rates. Enrichment factors ε(C) in chemostat (A) were determined according to eq 6 at different residual atrazine concentrations (B) resulting from decreasing dilution/growth rates (bar in lower panel B) (whiskers show 95% confidence intervals; N = 10). Enrichment factors observed in the absence of mass transfer limitations are drawn for comparison in panel (A): from degradation experiments with resting cells at high atrazine concentration,[32] of the pure enzyme,[35] and at high dilution in chemostat. Negative carbon enrichment factors reflect a normal isotope effect whereas positive nitrogen enrichment factors reflect an inverse isotope effect. Cell numbers are shown in panel (C), cell length and diameter, and cell volumes derived from panel (E) are shown in panel (D) (whiskers show the standard error; N = 50),. Images in (E) show typical bacterial cells observed during chemostat operation at the three dilution rates determined by phase contrast microscopy. Concentrations (B) and cell numbers (C) from one biological replicate are supported by data from a second biological replicate in SI Figure S6.

enzymatic reaction of TrzN. Since diffusion of atrazine through the media toward the cells can be ruled out considering the high agitation in the chemostat (600 rpm), the rate-limiting step of the degradation must be mass transfer across the cell membrane itself, in a similar way as conceptualized for cell membrane passage of CO_2 during algal growth.[21,23,24] Indeed, a common observation of these photosynthesis studies and our work is that isotope fractionation became smaller at lower concentrations of substrate: c[CO_2] in photosynthesis, c[atrazine] in our study. The difference between both studies, however, becomes evident when considering growth rate-to-substrate ratios (μ/c[CO_2]). While studies on algal photosynthesis consistently report a linear *increase* in isotope fractionation at lower μ/c[CO_2], in our experiments the opposite was observed: isotope fractionation *decreased* from ε(C) = −5.4‰ at higher μ/c[atrazine] = 0.29 $d^{-1}\mu M^{-1}$ (0.023 h^{-1}/0.38 μM) to ε(C) = −2.3‰ at lower μ_{min}/c[atrazine]$_{min}$ = 0.19 $d^{-1}\mu M^{-1}$ (0.006 h^{-1}/0.15 μM). How can this opposite trend be explained? In algal photosynthesis nitrate rather than CO_2 is the limiting nutrient. When growth rates μ are small, it is, therefore, because supply of nitrate is limited, not of CO_2. Hence, small μ/c[CO_2] makes for conditions in which CO_2 exchange between inside and outside the cell is maximized and carbon isotope fractionation is fully expressed. The situation is different in our experiments where small μ necessarily came along with mass transfer limitation of atrazine. In this case isotope fractionation *decreased* with lower μ/c[substrate]. Our results, therefore, imply that the relationship of μ/c[substrate] versus ε(C) brought forward for algal growth can only be expected if another nutrient (typically nitrate) is limiting because only then is ε(C) fully expressed when μ approaches zero, otherwise the same situation would be expected as in our experiments. It can also explain why this relationship was no longer observed in algal growth when nitrate limitation was alleviated (refs 21 and 23 and refs cited therein). Hence, our observation that isotope fractionation did not increase with lower growth rate, but that the opposite trend was observed, demonstrates that it was the low atrazine concentration that induced mass-transfer limitations, not variations in growth. Finally, we can also exclude changes in biomass as potential reason because cell densities remained constant irrespective of μ in our experiments.

Numerical Modeling Provides a Mass Transfer Estimate for Membrane Permeation. A numerical model was developed to provide quantitative estimates of the rates involved in the interplay between mass transfer limitation and degradation processes as described in Gharasoo et al.[44] In the absence of a mass transfer term, model predictions reproduced neither observed isotope ratios nor concentrations when based on Monod parameters derived from complementary experiments (Kundu et al., in communication): substrate affinity K_S = 237 ± 57 μg/L; maximum growth rate μ_{max} = 0.12 ± 0.02 h^{-1}. In contrast, the effect of masking on isotope ratios and concentrations could be adequately reproduced by implementing a linear mass transfer term with an estimated mass transfer coefficient of about k_{tr} = 0.0025 s^{-1} (Figure 3, SI Table S1). From this value of k_{tr} = 0.0025 s^{-1}, the diffusion coefficient through the membrane D_{mem} and the apparent permeability of the cell wall P_{app} calculate to P_{app} = 3.5 × 10^{-5} ms^{-1} and D_{mem} = 1.9 × 10^{-16} m^2s^{-1} (see theoretical treatment in the Experimental Section), which are values in a typical range of small organic molecules.[60] These conclusions are reinforced by model runs that included bacterial maintenance demand in the form of a Pirt type maintenance term.[50,61] As expected, the maintenance term had an effect on the biomass, but not on the

DOI: 10.1021/acs.est.8b05175
Environ. Sci. Technol. XXXX, XXX, XXX−XXX

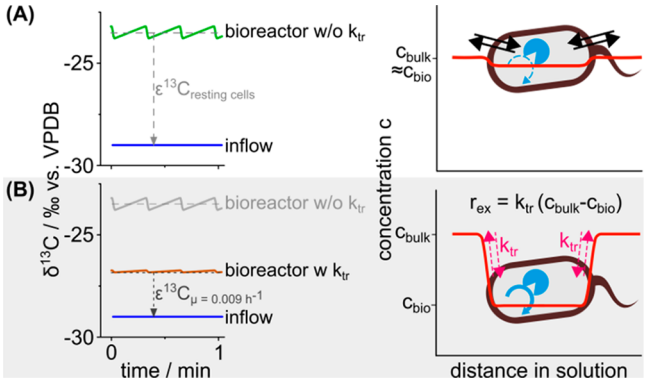

Figure 3. Numerical modeling validates the chemostat approach and delivers a first estimate of mass transfer rates. At low dilution rates, only few drops of medium per minute feed the culture so that degradation, and thus isotope enrichment of the substrate occurs in between drops. Numerical modeling demonstrates that the resulting oscillation of residual atrazine concentrations (Figure 1) and isotope ratios (Figure 3A) in chemostat lies within the uncertainty of ε-values thereby validating the chemostat approach to measure isotope fractionation. (A) In the absence of a mass transfer term the model predicts that carbon isotope values $\delta^{13}C$ inside the chemostat differ from those of the inflow by the enrichment factor $\varepsilon(C)$ of batch studies, independent of the dilution rate. (B) By incorporating a mass transfer term k_{tr} = 0.0025 s^{-1}, in contrast, simulated differences decrease to the same extent as observed in our experiments. The mass transfer limitation also predicts a concentration decrease inside the cell: modeled c_{bio} is only 40% of the concentration outside the cell, c_{bulk}.

phenomenon that isotope fractionation became smaller at low concentrations (SI Figures S7 and S8).

Adaptation of *A. aurescens* TC1 to Low Atrazine Concentrations. Interestingly, the evidence of mass transfer limitations was observed at a growth rate μ_{med} = 0.018 h^{-1} which is 16% of μ_{max} and the residual substrate concentration 61.5 μg/L is around 25% of K_S. In addition, we observed a fast onset of masked isotope fractionation within a remarkably small concentration range (from −5.36‰ at 83 μg/L to −2.12‰ at 44.5 μg/L), whereas a theoretical model by Thullner et al. predicts a slower onset over more than 1 order of magnitude in concentrations.[38] Growth under these low substrate concentrations is often accompanied by physiological changes to adapt to substrate limitation.[49,62] Indeed, we did observe changes in morphology as first indicator of physiological adaptation. While—with decreasing dilution rates—the number of live cells decreased (from 2.0 × 10^7 cells/mL to 1.4 × 10^7 cells/mL, Figure 2C), rod-shaped cells maintained their length (1.61 ± 0.05 μm), but increased their diameter (from 0.60 ± 0.02 μm at μ_{med} to 0.71 ± 0.01 μm at μ_{min}, Figure 2E) leading to a constant calculated dry weight at all dilution rates ($m_{biomass}$ = 0.56 ± 0.03 mg/L; SI Figure S3). This change from rod shape at high growth rates with atrazine in excess to coccus-like shape in stationary phase when atrazine concentrations are low in batch has also been described by Strong et al.[40] In chemostat cultivation the cells are still in a growing phase and the present observation of a change in morphology captures a transition from rod (high energy/high growth) to cocci (extreme low energy/no growth) shape and may be a strategy to minimize the bacterial surface-to-volume ratio to save energy. Considering that *A. aurescens* TC1 assimilates only five carbon atoms per atrazine molecule (7 mg_C/L),[40] the $m_{biomass}$ results in a yield of Y = 0.08 $g_{biomass}$/g_{carbon}, which is only 30% of that in fed-batch growth at high atrazine concentration (SI Figure S4). This observations suggests that a larger proportion of substrate goes into maintenance (no-growth associated reactions), which provides further evidence of physiological adaptation. Furthermore, as the low isotope fractionation reveals slow mass transfer compared to enzymatic turnover, this must inevitably lead to a depletion of substrate inside the cell. When describing this situation with the rate constants of the model, the intracellular substrate concentration (c_{bio}) is estimated to be reduced by 40% compared to those in solution (c_{bulk}) (3B). Hence, substrate scarcity inside the cell is more severe than apparent c_{bulk}. This is a promising starting point for future work to explore the consequences for physiological adaptation of *A. aurescens* TC1 to energy limitation.

Mass Transfer Limitations in Micropollutant Degradation Potentially Bias Assessments of Biodegradation with CSIA. The finding that growth under energy-limited conditions is accompanied by mass transfer limitations affects our understanding of contaminant biodegradation on multiple levels. Rate-limiting mass transfer across the cell membrane does not only slow down atrazine degradation in the environment but also masks the isotope fractionation of the underlying enzyme reaction. Specifically, since such isotope fractionation at low concentrations is smaller than measured in the lab at high pesticide concentrations, isotope-based assessments of biodegradation may become compromised in cases such as presented here. The extent of biodegradation in the environment would be underestimated for turnover of compounds at trace levels. As a consequence, the ideal strategy would include either (i) an estimate of the masking effects according to Thullner et al.'s model[38] or (ii) to directly measure possible mass transfer limitations by determining the enrichment factors in the laboratory at varying concentrations with our proposed chemostat approach instead of batch degradation experiments. Future studies may, therefore, show whether the findings of this study may be reproduced in other organisms.

Most importantly, our proof of concept provides a suitable experimental system to pinpoint this onset of possible mass transfer limitation for potentially a wide variety of bacterial strains and pollutants as growth-limiting substrates (with the only prerequisite that the underlying enzyme reaction must lead to pronounced isotope fractionation in a given element). In particular, the long cultivation times in chemostats allow bacterial adaptation to substrate limitation in atrazine degradation. In turn, this provides the unique opportunity to pinpoint the onset of mass transfer limitation for limiting substrates within a specific concentration range, and to study how microorganisms respond by employing specific adaptation strategies. Hence, future studies targeting (i) the maintenance energy and the threshold concentration at which adaptation is expected to take place and (ii) the role of physiological adaption to this substrate limitation, will be instrumental in shedding further light on limitations of micropollutant degradation at low concentrations.

■ ASSOCIATED CONTENT

Supporting Information

The Supporting Information is available free of charge on the ACS Publications website at DOI: 10.1021/acs.est.8b05175.

DOI: 10.1021/acs.est.8b05175
Environ. Sci. Technol. XXXX, XXX, XXX−XXX

A more detailed experimental section, graphs of additional *A. aurescens* TC1 cultivations and degradation experiments, the atrazine degradation pathway, and a table of modeled chemostat concentrations (PDF)

AUTHOR INFORMATION

Corresponding Authors

*(K.K.) E-mail: kankanakundu@gmail.com.

*(M.E.) Phone: +49 89 2180-78232; e-mail: m.elsner@tum.de.

ORCID

Martin Elsner: 0000-0003-4746-9052

Author Contributions

The manuscript was written through contributions of all authors. All authors have given approval to the final version of the manuscript.

Notes

The authors declare no competing financial interest.

ACKNOWLEDGMENTS

This work was funded by an ERC consolidator grant ("MicroDegrade", grant no. 616861) awarded by the European Research Council. We thank five anonymous reviewers for critical comments that helped improve the quality of the manuscript.

REFERENCES

(1) Martin Ruel, S.; Esperanza, M.; Choubert, J.-M.; Valor, I.; Budzinski, H.; Coquery, M. On-site evaluation of the efficiency of conventional and advanced secondary processes for the removal of 60 organic micropollutants. *Water Sci. Technol.* **2010**, *62* (12), 2970−2978.

(2) Dai, N.; Mitch, W. A. Relative Importance of N-Nitrosodimethylamine Compared to Total N-Nitrosamines in Drinking Waters. *Environ. Sci. Technol.* **2013**, *47* (8), 3648−3656.

(3) Barbieri, M.; Carrera, J.; Ayora, C.; Sanchez-Vila, X.; Licha, T.; Noedler, K.; Osorio, V.; Perez, S.; Koeck-Schulmeyer, M.; Lopez de Alda, M.; Barcelo, D. Formation of diclofenac and sulfamethoxazole reversible transformation products in aquifer material under denitrifying conditions: Batch experiments. *Sci. Total Environ.* **2012**, *426*, 256−263.

(4) Rosal, R.; Rodríguez, A.; Perdigón-Melón, J. A.; Petre, A.; García-Calvo, E.; Gómez, M. J.; Agüera, A.; Fernández-Alba, A. R. Occurrence of emerging pollutants in urban wastewater and their removal through biological treatment followed by ozonation. *Water Res.* **2010**, *44* (2), 578−588.

(5) Battaglin, W. A.; Meyer, M. T.; Kuivila, K. M.; Dietze, J. E. Glyphosate and Its Degradation Product AMPA Occur Frequently and Widely in U.S. Soils, Surface Water, Groundwater, and Precipitation. *J. Am. Water Resour. Assoc.* **2014**, *50* (2), 275−290.

(6) Ying, G. G.; Kookana, R. S.; Mallavarpu, M. Release behavior of triazine residues in stabilised contaminated soils. *Environ. Pollut.* **2005**, *134* (1), 71−77.

(7) Schwarzenbach, R. P.; Escher, B. I.; Fenner, K.; Hofstetter, T. B.; Johnson, C. A.; von Gunten, U.; Wehrli, B. The Challenge of Micropollutants in Aquatic Systems. *Science* **2006**, *313* (5790), 1072−1077.

(8) Tran, N. H.; Urase, T.; Ngo, H. H.; Hu, J.; Ong, S. L. Insight into metabolic and cometabolic activities of autotrophic and heterotrophic microorganisms in the biodegradation of emerging trace organic contaminants. *Bioresour. Technol.* **2013**, *146*, 721−731.

(9) Wu, M.; Quirindongo, M.; Sass, J.; Wetzler, A. *Still poisoning the well: atrazine continues to conatminate surface water and drinking water in the United States*; Natural Resources Defense Council: New York City, NY, 2010.

(10) Correia, F. V.; Macrae, A.; Guilherme, L. R. G.; Langenbach, T. Atrazine sorption and fate in a Ultisol from humid tropical Brazil. *Chemosphere* **2007**, *67* (5), 847−854.

(11) Egli, T. How to live at very low substrate concentration. *Water Res.* **2010**, *44* (17), 4826−4837.

(12) Button, D. K. Nutrient uptake by microorganisms according to kinetic parameters from theory as related to cytoarchitecture. *Microbiology and Molecular Biology Reviews* **1998**, *62* (3), 636.

(13) Ferenci, T.; Robert, K. P., Bacterial Physiology, Regulation and Mutational Adaptation in a Chemostat Environment. In *Advances in Microbial Physiology*; Academic Press, 2008; Vol. 53, pp 169−315.

(14) Bosma, T. N. P.; Middeldorp, P. J. M.; Schraa, G.; Zehnder, A. J. B. Mass Transfer Limitation of Biotransformation: Quantifying Bioavailability. *Environ. Sci. Technol.* **1997**, *31* (1), 248−252.

(15) Wick, A.; Wagner, M.; Ternes, T. A. Elucidation of the Transformation Pathway of the Opium Alkaloid Codeine in Biological Wastewater Treatment. *Environ. Sci. Technol.* **2011**, *45* (8), 3374−3385.

(16) Melander, L.; Saunders, W. H. *Reaction Rates of Isotopic Molecules*; John Wiley: New York, 1980; p 331.

(17) McKelvie, J. R.; Mackay, D. M.; de Sieyes, N. R.; Lacrampe-Couloume, G.; Sherwood Lollar, B. Quantifying MTBE biodegradation in the Vandenberg Air Force Base ethanol release study using stable carbon isotopes. *J. Contam. Hydrol.* **2007**, *94* (3−4), 157−165.

(18) Chartrand, M.; Passeport, E.; Rose, C.; Lacrampe-Couloume, G.; Bidleman, T. F.; Jantunen, L. M.; Lollar, B. S. Compound specific isotope analysis of hexachlorocyclohexane isomers: a method for source fingerprinting and field investigation of in situ biodegradation. *Rapid Commun. Mass Spectrom.* **2015**, *29* (6), 505−514.

(19) Braeckevelt, M.; Fischer, A.; Kästner, M. Field applicability of Compound-Specific Isotope Analysis (CSIA) for characterization and quantification of in situ contaminant degradation in aquifers. *Appl. Microbiol. Biotechnol.* **2012**, *94* (6), 1401−1421.

(20) Aeppli, C.; Berg, M.; Cirpka, O. A.; Holliger, C.; Schwarzenbach, R. P.; Hofstetter, T. B. Influence of Mass-Transfer Limitations on Carbon Isotope Fractionation during Microbial Dechlorination of Trichloroethene. *Environ. Sci. Technol.* **2009**, *43* (23), 8813−8820.

(21) Laws, E. A.; Popp, B. N.; Bidigare, R. R.; Riebesell, U.; Burkhardt, S.; Wakeham, S. G., Controls on the molecular distribution and carbon isotopic composition of alkenones in certain haptophyte algae. *Geochem., Geophys., Geosyst.* **2001**, *2*, (1).n/a

(22) O'Leary, M. H. Carbon Isotopes in Photosynthesis. *BioScience* **1988**, *38* (5), 328−336.

(23) Wilkes, E. B.; Carter, S. J.; Pearson, A. CO2-dependent carbon isotope fractionation in the dinoflagellate Alexandrium tamarense. *Geochim. Cosmochim. Acta* **2017**, *212*, 48−61.

(24) Laws, E. A.; Popp, B. N.; Bidigare, R. R.; Kennicutt, M. C.; Macko, S. A. Dependence of phytoplankton carbon isotopic composition on growth rate and [CO2)aq: Theoretical considerations and experimental results. *Geochim. Cosmochim. Acta* **1995**, *59* (6), 1131−1138.

(25) Brunner, B.; Bernasconi, S. M.; Kleikemper, J.; Schroth, M. H. A model for oxygen and sulfur isotope fractionation in sulfate during bacterial sulfate reduction processes. *Geochim. Cosmochim. Acta* **2005**, *69* (20), 4773−4785.

(26) Wing, B. A.; Halevy, I. Intracellular metabolite levels shape sulfur isotope fractionation during microbial sulfate respiration. *Proc. Natl. Acad. Sci. U. S. A.* **2014**, *111* (51), 18116−18125.

(27) Kritee, K.; Sigman, D. M.; Granger, J.; Ward, B. B.; Jayakumar, A.; Deutsch, C. Reduced isotope fractionation by denitrification under conditions relevant to the ocean. *Geochim. Cosmochim. Acta* **2012**, *92* (0), 243−259.

(28) Wunderlich, A.; Heipieper, H. J.; Elsner, M.; Einsiedl, F. Solvent stress-induced changes in membrane fatty acid composition of denitrifying bacteria reduce the extent of nitrogen stable isotope fractionation during denitrification. *Geochim. Cosmochim. Acta* **2018**, *239*, 275−283.

DOI: 10.1021/acs.est.8b05175
Environ. Sci. Technol. XXXX, XXX, XXX−XXX

(29) Ehrl, B. N.; Mogusu, E. O.; Kim, K.; Hofstetter, H.; Pedersen, J. A.; Elsner, M. High Permeation Rates in Liposome Systems Explain Rapid Glyphosate Biodegradation Associated with Strong Isotope Fractionation. *Environ. Sci. Technol.* **2018**, *52* (13), 7259−7268.
(30) Ehrl, B. N.; Gharasoo, M.; Elsner, M. Isotope Fractionation Pinpoints Membrane Permeability as a Barrier to Atrazine Biodegradation in Gram-negative Polaromonas sp. Nea-C. *Environ. Sci. Technol.* **2018**, *52* (7), 4137−4144.
(31) Farquhar, G. D.; Ehleringer, J. R.; Hubick, K. T. Carbon Isotope Discrimination and Photosynthesis. *Annu. Rev. Plant Physiol. Plant Mol. Biol.* **1989**, *40*, 503−537.
(32) Meyer, A. H.; Penning, H.; Elsner, M. C and N isotope fractionation suggests similar mechanisms of microbial atrazine transformation despite involvement of different Enzymes (AtzA and TrzN). *Environ. Sci. Technol.* **2009**, *43* (21), 8079−8085.
(33) Reinnicke, S.; Simonsen, A.; Sørensen, S. R.; Aamand, J.; Elsner, M. C and N Isotope Fractionation during Biodegradation of the Pesticide Metabolite 2,6-Dichlorobenzamide (BAM): Potential for Environmental Assessments. *Environ. Sci. Technol.* **2012**, *46* (3), 1447−1454.
(34) Clingenpeel, S. R.; Moan, J. L.; McGrath, D. M.; Hungate, B. A.; Watwood, M. E. Stable carbon isotope fractionation in chlorinated ethene degradation by bacteria expressing three toluene oxygenases. *Front. Microbiol.* **2012**, *3*, 63.
(35) Schürner, H. K. V.; Seffernick, J. L.; Grzybkowska, A.; Dybala-Defratyka, A.; Wackett, L. P.; Elsner, M. Characteristic Isotope Fractionation Patterns in s-Triazine Degradation Have Their Origin in Multiple Protonation Options in the s-Triazine Hydrolase TrzN. *Environ. Sci. Technol.* **2015**, *49* (6), 3490−3498.
(36) Renpenning, J.; Rapp, I.; Nijenhuis, I. Substrate hydrophobicity and cell composition influence the extent of rate limitation and masking of isotope fractionation during microbial reductive dehalogenation of chlorinated ethenes. *Environ. Sci. Technol.* **2015**, *49* (7), 4293−4301.
(37) Kampara, M.; Thullner, M.; Richnow, H. H.; Harms, H.; Wick, L. Y. Impact of Bioavailability Restrictions on Microbially Induced Stable Isotope Fractionation. 2. Experimental Evidence. *Environ. Sci. Technol.* **2008**, *42* (17), 6552−6558.
(38) Thullner, M.; Kampara, M.; Richnow, H. H.; Harms, H.; Wick, L. Y. Impact of Bioavailability Restrictions on Microbially Induced Stable Isotope Fractionation. 1. Theoretical Calculation. *Environ. Sci. Technol.* **2008**, *42* (17), 6544−6551.
(39) Elsner, M.; Imfeld, G. Compound-specific isotope analysis (CSIA) of micropollutants in the environment — current developments and future challenges. *Curr. Opin. Biotechnol.* **2016**, *41*, 60−72.
(40) Strong, L. C.; Rosendahl, C.; Johnson, G.; Sadowsky, M. J.; Wackett, L. P. *Arthrobacter aurescens* TC1 metabolizes diverse s-triazine ring compounds. *Appl. Environ. Microbiol.* **2002**, *68* (12), 5973−5980.
(41) Sajjaphan, K.; Shapir, N.; Wackett, L. P.; Palmer, M.; Blackmon, B.; Sadowsky, M. J. *Arthrobacter aurescens* TC1 atrazine catabolism genes trzN, atzB, and atzC are linked on a 160-kilobase region and are functional in *Escherichia coli*. *Appl. Environ. Microbiol.* **2004**, *70* (7), 4402−4407.
(42) Martinez, B.; Tomkins, J.; Wackett, L. P.; Wing, R.; Sadowsky, M. J. Complete Nucleotide Sequence and Organization of the Atrazine Catabolic Plasmid pADP-1 from *Pseudomonas* sp Strain ADP. *J. Bacteriol.* **2001**, *183* (19), 5684−5697.
(43) Devers, M.; Soulas, G.; Martin-Laurent, F. Real-time reverse transcription PCR analysis of expression of atrazine catabolism genes in two bacterial strains isolated from soil. *J. Microbiol. Methods* **2004**, *56* (1), 3−15.
(44) Gharasoo, M.; Ehrl, B. N.; Cirpka, O. A.; Elsner, M., Modeling of contaminant biodegradation and compound-specific isotope fractionation in chemostats at low dilution rates. *Environ. Sci. Technol.* **2018** DOI: 10.1021/acs.est.8b02498
(45) Best, J. B. The inference of intracellular enzymatic properties from kinetic data obtained on living cells. I. Some kinetic considerations regarding an enzyme enclosed by a diffusion barrier. *J. Cell. Comp. Physiol.* **1955**, *46* (1), 1−27.
(46) Stenzel, A.; Goss, K. U.; Endo, S. Determination of Polyparameter Linear Free Energy Relationship (pp-LFER) Substance Descriptors for Established and Alternative Flame Retardants. *Environ. Sci. Technol.* **2013**, *47* (3), 1399.
(47) Van Meer, G.; Voelker, D. R.; Feigenson, G. W. Membrane lipids: where they are and how they behave. *Nat. Rev. Mol. Cell Biol.* **2008**, *9* (2), 112−124.
(48) Hoefs, J., Theoretical and Experimental Principles. In *Stable Isotope Geochemistry*, 3rd ed.; Wyllie, P. J., Ed.; Springer-Verlag: Chicago, 1987; pp 1−25.
(49) Trautwein, K.; Lahme, S.; Wöhlbrand, L.; Feenders, C.; Mangelsdorf, K.; Harder, J.; Steinbüchel, A.; Blasius, B.; Reinhardt, R.; Rabus, R. Physiological and Proteomic Adaptation of *Aromatoleum aromaticum* EbN1 to Low Growth Rates in Benzoate-Limited, Anoxic Chemostats. *J. Bacteriol.* **2012**, *194* (9), 2165−2180.
(50) Kovarova-Kovar, K.; Egli, T. Growth kinetics of suspended microbial cells: From single-substrate-controlled growth to mixed-substrate kinetics. *Microbiology and Molecular Biology Reviews* **1998**, *62* (3), 646.
(51) Coplen, T. B. Guidelines and recommended terms for expression of stable-isotope-ratio and gas-ratio measurement results. *Rapid Commun. Mass Spectrom.* **2011**, *25* (17), 2538−2560.
(52) Schreglmann, K.; Hoeche, M.; Steinbeiss, S.; Reinnicke, S.; Elsner, M. Carbon and nitrogen isotope analysis of atrazine and desethylatrazine at sub-microgram per liter concentrations in groundwater. *Anal. Bioanal. Chem.* **2013**, *405* (9), 2857−2867.
(53) Münster, U. Concentrations and fluxes of organic carbon substrates in the aquatic environment. *Antonie van Leeuwenhoek* **1993**, *63* (3−4), 243−274.
(54) Graymore, M.; Stagnitti, F.; Allinson, G. Impacts of atrazine in aquatic ecosystems. *Environ. Int.* **2001**, *26* (7−8), 483−495.
(55) Davidson, M. M.; Bisher, M. E.; Pratt, L. M.; Fong, J.; Southam, G.; Pfiffner, S. M.; Reches, Z.; Onstott, T. C. Sulfur Isotope Enrichment during Maintenance Metabolism in the Thermophilic Sulfate-Reducing Bacterium Desulfotomaculum putei. *Appl. Environ. Microbiol.* **2009**, *75* (17), 5621−5630.
(56) Penning, H.; Plugge, C. M.; Galand, P. E.; Conrad, R. Variation of carbon isotope fractionation in hydrogenotrophic methanogenic microbial cultures and environmental samples at different energy status. *Global Change Biology* **2005**, *11* (12), 2103−2113.
(57) Penning, H.; Conrad, R. Effect of inhibition of acetoclastic methanogenesis on growth of archaeal populations in an anoxic model environment. *Appl. Environ. Microbiol.* **2006**, *72* (1), 178−184.
(58) Hayes, J. M. Fractionation of carbon and hydrogen isotopes in biosynthetic processes. *Rev. Mineral. Geochem.* **2001**, *43*, 225−277.
(59) Schmidt, T. C.; Zwank, L.; Elsner, M.; Berg, M.; Meckenstock, R. U.; Haderlein, S. B. Compound-specific stable isotope analysis of organic contaminants in natural environments: a critical review of the state of the art, prospects, and future challenges. *Anal. Bioanal. Chem.* **2004**, *378* (2), 283−300.
(60) Males, R. G.; Herring, F. G. A 1H-NMR study of the permeation of glycolic acid through phospholipid membranes. *Biochim. Biophys. Acta, Biomembr.* **1999**, *1416* (1−2), 333−338.
(61) Pirt, S. J. The maintenance energy of bacteria in growing cultures. *Proc. R. Soc. London, Ser. B* **1965**, *163* (991), 224−231.
(62) Marozava, S.; Röling, W. F.; Seifert, J.; Küffner, R.; Von Bergen, M.; Meckenstock, R. U. Physiology of *Geobacter metallireducens* under excess and limitation of electron donors. Part II. Mimicking environmental conditions during cultivation in retentostats. *Syst. Appl. Microbiol.* **2014**, *37* (4), 287−295.

NOTE ADDED AFTER ASAP PUBLICATION

Due to a production oversight, this article published December 19, 2018 with an error in equation 1. The correct equation published December 20, 2018.

DOI: 10.1021/acs.est.8b05175
Environ. Sci. Technol. XXXX, XXX, XXX−XXX